



Universidad Autónoma
de Madrid

Biblos-e Archivo
Repositorio Institucional UAM

Repositorio Institucional de la Universidad Autónoma de Madrid
<https://repositorio.uam.es>

Esta es la **versión de autor** del artículo publicado en:
This is an **author produced version** of a paper published in:

Neurocomputing 275 (2018): 818-828

DOI: <https://doi.org/10.1016/j.neucom.2017.09.025>

Copyright: © 2017. This manuscript version is made available under the
CC-BY-NC-ND 4.0 licence <http://creativecommons.org/licenses/by-nc-nd/4.0/>

El acceso a la versión del editor puede requerir la suscripción del recurso
Access to the published version may require subscription

Bayesian Optimization of a Hybrid System for Robust Ocean Wave Features Prediction

L. Cornejo-Bueno^a, E. C. Garrido-Merchán^b, D. Hernández-Lobato^b, S.
Salcedo-Sanz^{a,c}

^a*Department of Signal Processing and Communications, Universidad de Alcalá, 28805
Alcalá de Henares, Madrid, Spain.*

^b*Computer Science Department, Universidad Autónoma de Madrid, 28049, Madrid,
Spain.*

^c*Corresponding author: Sancho Salcedo Sanz. email: sancho.salcedo@uah.es*

Abstract

In the last years, Bayesian optimization (BO) has emerged as a practical tool for high-quality parameter selection in prediction systems. BO methods are useful for optimizing black-box objective functions that either lack an analytical expression, or are very expensive to evaluate. In this paper we show that BO can be used to obtain the optimal parameters of a prediction system for problems related to ocean wave features prediction. Specifically, we propose the Bayesian optimization of a hybrid Grouping Genetic Algorithm for attribute selection combined with an Extreme Learning Machine (GGA-ELM) approach for prediction. The system uses data from neighbor stations (usually buoys) in order to predict the significant wave height and the wave energy flux at a goal marine structure facility. The proposed BO methodology has been tested in a real problem involving buoys data in the Western coast of the USA, improving the performance of the GGA-ELM without a BO approach.

Keywords: Ocean waves features; Prediction System; Bayesian optimization.

1. Introduction

The accurate prediction of waves features plays a key role in different ocean engineering-related activities, such as safe ship navigation [1, 2], the design of marine structures [3, 4], *e.g.*, oil platforms and harbours, and in

17 marine energy management problems [5, 6], like the proper operation of wave
18 energy converters [7], among others. Thus, the topic has a clear impact on
19 human safety, economics and clean energy production. One of the most
20 important features to define the severity of a given ocean wave field is the
21 significant wave height, H_{m_0} . H_{m_0} is usually estimated using in-situ sensors,
22 such as buoys, recording time series of wave elevation information. Buoys
23 provide reliable sea state information that characterizes the wave field in a
24 fixed position (i.e. the mooring point). In addition, as buoys are anchored in
25 a hostile media (the ocean), the probability that measuring problems (and
26 therefore missing data) occur in situations of severe weather is very high [8].
27 Besides this, marine energy [9, 10] is currently one of the most promising
28 sources of renewable energy, still minor at a global level, but playing a major
29 role in several offshore islands [11, 12]. In this case, the accurate estimation of
30 the wave energy flux P is relevant to characterize the wave energy production
31 from Wave Energy Converters (WECs) facilities [13].

32 The research work on wave features prediction systems has been intense
33 in the last years, with special incidence in machine learning approaches.
34 One of the first works on this topic was the direct prediction of H_{m_0} using
35 artificial neural networks in [14]. Improvements on this prediction system
36 were further presented in [15]. Neural networks have also been applied to
37 other problems of H_{m_0} and P prediction, such as [16], where H_{m_0} and P
38 are inferred from observed wave records using time series neural networks.
39 In [17] neural networks were applied to estimate the final breaking wave-
40 height for laboratory-scaled and full-scaled ocean waves, showing that neural
41 models are able to improve previously proposed empirical models for breaking
42 waves-height estimation in terms of accuracy. In [18] a neural network was
43 applied to estimate the wave energy resource in the northern coast of Spain.
44 In [19] a hybrid genetic algorithm-adaptive network-based fuzzy inference
45 system model was developed to forecast H_{m_0} and the peak spectral period
46 at Lake Michigan. In [20] and [21] different hybrid algorithms mixed with an
47 Extreme Learning Machine neural network were proposed for the estimation
48 of H_{m_0} and P , in the context of marine energy applications. Alternative
49 methods based on different computational approaches have been recently
50 proposed. For example, in [22] different soft-computing techniques are tested
51 for H_{m_0} prediction. Support Vector regression (SVR) has also been applied
52 to marine energy related problems such as in [23]. Similarly, [24] and [25]
53 proposed to feed SVR approaches with information from radar sources in
54 order to obtain an accurate prediction of H_{m_0} and P features. Classification

55 approaches have been applied in [26] to analyze and predict H_{m_0} and P ranges
56 in buoys for marine energy applications. In [27], use of genetic programming
57 for H_{m_0} reconstruction problems was proposed. Finally, in [28] fuzzy logic-
58 based approaches were introduced for H_{m_0} prediction problems.

59 In this paper we test a BO methodology to improve the performance
60 of a hybrid prediction system for wave features (H_{m_0} and P) prediction.
61 Specifically, the prediction system was previously presented in [21], and it
62 is formed by a Grouping Genetic Algorithm for feature selection, and an
63 Extreme Learning Machine for carrying out the final energy flux prediction.
64 This hybrid prediction system has a number of parameters that may affect
65 its final performance, and need to be previously specified by the practitioner.
66 Traditionally, these parameters have been manually tuned by a human ex-
67 pert, with experience in both the algorithm and the problem domain. How-
68 ever, it is possible to obtain better results by an automatic fine tuning of the
69 prediction system's parameters. In this case, the parameters of GGA-ELM
70 approach include the probability of mutation in the GGA or the number of
71 neurons in the ELM hidden layer, among others. We propose then to use a
72 Bayesian optimization (BO) approach to automatically optimize the param-
73 eters of the whole prediction system (GGA-ELM), with the aim of improving
74 its performance in wave energy prediction problems. BO has been shown
75 to obtain good results in the task of obtaining good parameter values for
76 prediction systems [29]. In the paper we detail the basic prediction system
77 considered and the BO methodology implemented, along with the improve-
78 ments obtained in real problems of H_{m_0} and P prediction in the Western
79 coast of the USA.

80 The rest of the paper is organized as follows: the next section details
81 the calculation of the features of interest in ocean wave characterization,
82 H_{m_0} and P in this case. Section 3 describes the main characteristics of the
83 hybrid system to be optimized, which is formed by a GGA and an ELM
84 for prediction. Section 4 presents the Bayesian optimization methodology
85 applied in this case to optimize the prediction system considered. Section 5
86 presents the experimental part of the paper, where the Bayesian hybrid GGA-
87 ELM approach is tested in a real problem of P prediction in the Western coast
88 of the USA. Finally, Section 6 closes the paper exposing the conclusions of
89 this work.

90 **2. Wave features of interest: calculation of H_{m_0} and P**

91 In the evaluation of marine systems it is essential to previously character-
92 ize as accurately as possible the wave features of the zone under study. For
93 example, in a wave energy facility, it is necessary to characterize the amount
94 of wave energy available at a particular location, which is given by features
95 such as H_{m_0} and P . In order to obtain these features, it is necessary to focus
96 on the water surface, and within the framework of the linear wave theory,
97 the vertical wave elevation, $\eta(\mathbf{r}, t)$, at a point $\mathbf{r} = (x, y)$ on the sea surface at
98 time t can be assumed as a superposition of different monochromatic wave
99 components [30, 31]. This model is appropriate when the free wave compo-
100 nents do not vary appreciably in space and time (that is, statistical temporal
101 stationarity and spatial homogeneity can be assumed [31]).

102 In the model described, the concept of “sea state” refers to the sea area
103 and the time interval in which the statistical and spectral characteristics of
104 the wave do not change considerably (statistical temporal stationarity and
105 spatial homogeneity). The features of a given sea state are then the com-
106 bined contribution of all features from different sources. For example, the
107 “wind sea” occurs when the waves are caused by the energy transferred be-
108 tween the local wind and the free surface of the sea. The “swell” is the
109 situation in which the waves have been generated by winds blowing on an-
110 other far area (for instance, by storms), and propagate towards the region
111 of observation. Usually, sea states are the composition of these two pure
112 states, forming multi-modal or mixed seas. In a given sea state, the wave
113 elevation $\eta(\mathbf{r}, t)$ with respect to the mean ocean level can be assumed as a
114 *zero-mean Gaussian stochastic process*, with statistical symmetry between
115 wave maxima and minima. A buoy deployed at point \mathbf{r}_B can take samples
116 of this process, $\eta(\mathbf{r}_B, t_j)$ $j = 1, 2, \dots, t_{\text{MAX}}$, generating thus a time series of
117 empirical vertical wave elevations. The Discrete Fourier Transform (DFT) of
118 this sequence, using the Fast Fourier Transform (FFT) algorithm, allows for
119 estimating the *spectral density* $S(f)$. Its spectral moments of order n can be
120 computed as follows:

$$m_n = \int_0^\infty f^n S(f) df. \quad (1)$$

121 The Significant Wave Height (SWH) is defined as the average (in meters)
122 of the highest one-third of all the wave heights during a 20-minute sampling

123 period [32], and it has been widely studied. It can be calculated from the
 124 moment of order 0 in Equation (1), as follows:

$$H_{m_0} = 4 \cdot (m_0)^{1/2}. \quad (2)$$

125 On the other hand, the wave energy flux is a first indicator of the amount
 126 of wave energy available in a given area of the ocean. Wave energy flux P ,
 127 or power density per meter of wave crest [33] can be computed as

$$P = \frac{\rho g^2}{4\pi} \int_0^\infty \frac{S(f)}{f} df = \frac{\rho g^2}{4\pi} m_{-1} = \frac{\rho g^2}{64\pi} H_{m_0}^2 \cdot T_e, \quad (3)$$

128 where ρ is the sea water density (1025 kg/m³), g is the acceleration due to
 129 gravity, $H_{m_0} = 4\sqrt{m_0}$ is the spectral estimation of the significant wave height,
 130 and $T_e \equiv T_{-1,0} = m_{-1}/m_0$ is an estimation of the mean wave period, normally
 131 known as the period of energy, which is used in the design of turbines for wave
 132 energy conversion. Expression (3) (with H_{m_0} in meters and T_e in seconds)
 133 leads to

$$P = 0.49 \cdot H_{m_0}^2 \cdot T_e, \quad (4)$$

134 measured in kW/m , which helps engineers estimate the amount of wave
 135 energy available when planning the deployment of WECs at a given location.

136 3. The hybrid prediction system considered

137 In this paper we will optimize a hybrid prediction system for marine en-
 138 ergy applications described in [25]. In this section we describe the main char-
 139 acteristics of this approach, in order to better explain later on the Bayesian
 140 optimization carried out on it. The prediction system is a hybrid wrapper
 141 approach, formed by a Grouping Genetic Algorithm for feature selection, and
 142 an Extreme Learning Machine to carry out the final prediction of H_{m_0} or P
 143 from a set of input data.

144 3.1. The Grouping Genetic Algorithm

145 The grouping genetic algorithm (GGA) [34, 35] is a type of evolution-
 146 ary algorithm especially suited to tackle grouping problems, i.e., problems
 147 where a number of items must be assigned to a set of predefined groups.
 148 The GGA has shown very good performance on different real applications
 149 and problems [36, 37, 38, 39, 40, 41]. In the GGA, the encoding, crossover

150 and mutation operators of traditional GAs are modified to better deal with
 151 grouping problems. In this paper we use the GGA to obtain a reduced set
 152 of features (feature selection) in a context of H_{m_0} and P prediction. We
 153 structure the description of the GGA in Encoding, Operators and Fitness
 154 Function calculation (Extreme Learning Machine).

155 3.1.1. Problem encoding

156 The GGA is a variable-length genetic algorithm. The encoding is defined
 157 by separating each individual in the algorithm into two parts: an *assign-*
 158 *ment* part, which associates each item to a given group, and a *group* part,
 159 which defines the groups that must be taken into account for the individ-
 160 ual. In problems where the number of groups is not previously defined, it
 161 is straightforward that this is a variable-length algorithm: the group part
 162 varies from one individual to another. In our implementation of the GGA
 163 for feature selection, an individual \mathbf{c} has the form $\mathbf{c} = [\mathbf{a}|\mathbf{g}]$. An example of
 164 an individual in the proposed GGA for a feature selection problem, with 20
 165 features and 4 groups, is the following:

166 1 1 2 3 1 4 1 4 3 4 4 1 2 4 4 2 3 1 3 2 | 1 2 3 4

167 where the group 1 includes features $\{1, 2, 5, 7, 12, 18\}$, group 2 features
 168 $\{3, 13, 16, 20\}$, group 3 features $\{4, 9, 17, 19\}$ and finally group 4 includes fea-
 169 tures $\{6, 8, 10, 11, 14, 15\}$.

170 3.1.2. Genetic operators

171 In this paper we use a tournament-based selection mechanism, similar to
 172 the one described in [42]. This mechanism has been shown to be one of the
 173 most effective selection operators, avoiding super-individuals and performing
 174 a excellent exploration of the search space. Regarding the crossover operator,
 175 we have chosen a modified version of the one initially proposed by Falkenauer
 176 [34, 35]. It follows the process outlined in Figure 1:

- 177 1. Choose two parents from the current population, at random.
- 178 2. Randomly select two points for the crossover, from the “Groups” part of
 179 parent 1, then, all the groups between the two cross-points are selected.
 180 In the example of Figure 1 the two crossover points are G_1 and G_2 . Note
 181 that, in this case the items of parent1 belonging to group G_1 and G_2
 182 are 1, 2, 4, 5, and 6.

- 183 3. Insert the selected section of the “Groups” part into the second parent.
 184 After the insertion in the example of Figure 1, the assignment of the
 185 nodes 1, 2, 4, 5 and 6 of the offspring individual will be those of parent
 186 1, while the rest of the nodes’ assignment are those of parent 2. The
 187 “Groups” part of the offspring individual is that of parent 2 plus the
 188 selected section of parent 1 (8 groups in total, in this case).
- 189 4. Modify the “Groups” part of the offspring individual with their corre-
 190 sponding number. In the example, $G = 1\ 2\ 3\ 4\ 5\ 6\ 1\ 2$ is
 191 modified into $G = 1\ 2\ 3\ 4\ 5\ 6\ 7\ 8$. Modify also the assignment
 192 part accordingly.
- 193 5. Remove any empty groups in the offspring individual. In the example
 194 considered, it is found that groups 1, 2, 3, and 6 are empty, so we can
 195 eliminate these groups identification number and rearrange the rest.
 196 The final offspring is then obtained.

197 Regarding mutation operator, we apply a swapping mutation in which
 198 two items are interchanged (swapping this way the assignment of features to
 199 different groups). This procedure is carried out with a very low probability
 200 ($P_m = 0.01$), to avoid increasing of the random search in the process. In the
 201 next section we describe the fitness function used to guide the search in the
 202 GGA, the ELM neural network, which is a very fast algorithm with excellent
 203 performance in prediction problems.

204 3.1.3. Fitness function: the Extreme Learning Machine

205 An ELM [43] is a fast learning method based on the structure of MLPs
 206 with a novel way of training feed-forward neural networks. One of the most
 207 important characteristics of the ELM training is the randomness in the pro-
 208 cess where the network weights are set, obtaining, in this way, a pseudo-
 209 inverse of the hidden-layer output matrix. The simplicity of this technique
 210 makes the training algorithm extremely fast. Moreover, it is remarkable the
 211 outstanding performance shown when compared to other learning methods.
 212 For example, it usually outperforms other established approaches such as
 213 classical MLPs or SVRs [43]. ELMs have recently been used within hybrid
 214 wrapper systems for feature selection [44, 45], similarly as we use them in
 215 this paper.

The ELM algorithm can be explained as follows: given a training set

$$\mathbb{T} = (\mathbf{x}_i, \mathbf{W}_i) | \mathbf{x}_i \in \mathbb{R}^n, \mathbf{W}_i \in \mathbb{R}, i = 1, \dots, l,$$

216 an activation function $g(x)$ and number of hidden nodes (\tilde{N}),

- 217 1. Randomly assign inputs weights \mathbf{w}_i and bias b_i , $i = 1, \dots, \tilde{N}$.
- 218 2. Calculate the hidden layer output matrix \mathbf{H} , defined as

$$\mathbf{H} = \begin{bmatrix} g(\mathbf{w}_1 \mathbf{x}_1 + b_1) & \cdots & g(\mathbf{w}_{\tilde{N}} \mathbf{x}_1 + b_{\tilde{N}}) \\ \vdots & \cdots & \vdots \\ g(\mathbf{w}_1 \mathbf{x}_l + b_1) & \cdots & g(\mathbf{w}_{\tilde{N}} \mathbf{x}_N + b_{\tilde{N}}) \end{bmatrix}_{l \times \tilde{N}}. \quad (5)$$

- 219 3. Calculate the output weight vector β as

$$\beta = \mathbf{H}^\dagger \mathbf{T}, \quad (6)$$

220 where \mathbf{H}^\dagger stands for the Moore-Penrose inverse of matrix \mathbf{H} [43], and
221 \mathbf{T} is the training output vector, $\mathbf{T} = [\mathbf{W}_1, \dots, \mathbf{W}_l]^T$.

222 The number of hidden nodes (\tilde{N}) is a free parameter of the ELM training,
223 and it can be fixed initially, or in a best convenient way, it must be estimated
224 for obtaining good results as a part of a validation set in the learning process.
225 Hence, scanning a range of \tilde{N} values is the solution for this problem.

226 The Matlab ELM implementation by G. B. Huang, freely available on
227 the Internet [46], has been used in this paper.

228 4. Bayesian optimization of the prediction system

229 Every machine learning algorithm or prediction system has its own set
230 of parameters that must be adjusted to obtain an optimal performance. An
231 example is a deep neural network in which one has to specify parameters
232 such as the learning rate, the number of layers, the number of neurons in
233 each layer, etc. [47]. Another example is stochastic gradient boosting in
234 which one has to choose the number of terminal nodes in the ensemble trees,
235 the number of trees, the regularization parameter, etc. [48]. In our particular
236 setting, in an ELM the number of units in the hidden layer has to be specified
237 before training; and in the genetic algorithm described in Section 3.1, the
238 probability of mutation and the number of epochs must be known initially.

239 Changing the parameter values of a prediction system may have a strong
240 impact in its performance. Parameter tuning is hence defined as the problem
241 of finding the optimal parameter values of a prediction system on the problem
242 considered. This task has traditionally been addressed by human experts,

243 which often use prior knowledge to specify parameter values that are expected
244 to perform well. However, such an approach can suffer from human bias.
245 An alternative solution is to consider a grid or uniform search in the space
246 of parameters to look for values that result in a good performance on a
247 validation set. These methods, however, suffer when the dimensionality of
248 the parameter space is very high [49]. In those settings they often require a
249 large number of parameter evaluations.

250 Bayesian optimization (BO) has emerged as practical tool for parameter
251 selection in prediction systems. These methods provide an efficient alterna-
252 tive to a grid or uniform search of the parameter space [29]. Assume that
253 the surface defined by the error of a prediction system that depends on some
254 parameters is smooth. In that case, we can search through the parameter
255 space according to a criterion that exploits this smoothness property and
256 avoids exhaustive exploration. More precisely, BO methods are very useful
257 for optimizing black-box objective functions that lack an analytical expres-
258 sion (which means no gradient information), are very expensive to evaluate,
259 and in which the evaluations are potentially noisy [50, 51, 52]. The perfor-
260 mance of a prediction system on a randomly chosen validation set, when seen
261 as a function of the chosen parameters, has all these characteristics.

262 Consider a black-box objective $f(\cdot)$ with noisy evaluations of the form
263 $y_i = f(\mathbf{x}_i) + \epsilon_i$, with ϵ_i some noise term. BO methods are very successful at
264 reducing the number of evaluations of the objective function needed to solve
265 the optimization problem. At each iteration $t = 1, 2, 3, \dots$ of the optimiza-
266 tion process, these methods fit a probabilistic model, typically a Gaussian
267 process (GP) to the observations of objective function $\{y_i\}_{i=1}^{t-1}$ collected so
268 far. The uncertainty about the objective function provided by the GP is then
269 used to generate an acquisition function $\alpha(\cdot)$, whose value at each input lo-
270 cation indicates the expected utility of evaluating $f(\cdot)$ there. The next point
271 \mathbf{x}_t at which to evaluate the objective $f(\cdot)$ is the one that maximizes $\alpha(\cdot)$.
272 Importantly, $\alpha(\cdot)$ only depends on the probabilistic model and can hence be
273 evaluated with very little cost. Thus, this function can be maximized very
274 quickly using standard optimization techniques. This process is repeated
275 until enough data about the objective has been collected. When this is the
276 case, the GP predictive mean for $f(\cdot)$ can be optimized to find the solution of
277 the optimization problem. Algorithm 1 shows the details of such a process.

The key for BO success is that evaluating the acquisition function $\alpha(\cdot)$ is
very cheap compared to the evaluation of the actual objective $f(\cdot)$, which in
our case requires re-training the prediction system. This is so because the

for $t = 1, 2, 3, \dots, \text{max_steps}$ **do**

- 1:** Find the next point to evaluate by optimizing the acquisition function: $\mathbf{x}_t = \arg \max_{\mathbf{x}} \alpha(\mathbf{x} | \mathcal{D}_{1:t-1})$.
- 2:** Evaluate the black-box objective $f(\cdot)$ at \mathbf{x}_t : $y_t = f(\mathbf{x}_t) + \epsilon_t$.
- 3:** Augment the observed data $\mathcal{D}_{1:t} = \mathcal{D}_{1:t-1} \cup \{\mathbf{x}_t, y_t\}$.
- 4:** Update the Gaussian process model using $\mathcal{D}_{1:t}$.

end

Result: Optimize the mean of the Gaussian process to find the solution.

Algorithm 1: Bayesian optimization of a black-box objective function.

acquisition function only depends on the GP predictive distribution for $f(\cdot)$ at a candidate point \mathbf{x} . Let the observed data until step $t - 1$ of the algorithm be $\mathcal{D}_i = \{(\mathbf{x}_i, y_i)\}_{i=1}^{t-1}$. The GP predictive distribution for $f(\cdot)$ is given by a Gaussian distribution characterized by a mean $\mu(\mathbf{x})$ and a variance $\sigma^2(\mathbf{x})$. These values are:

$$\mu(\mathbf{x}) = \mathbf{k}_*^T (\mathbf{K} + \sigma_n^2 I)^{-1} \mathbf{y}, \quad (7)$$

$$\sigma^2(\mathbf{x}) = k(\mathbf{x}, \mathbf{x}) - \mathbf{k}_*^T (\mathbf{K} + \sigma_n^2 I)^{-1} \mathbf{k}_*. \quad (8)$$

278 where $\mathbf{y} = (y_1, \dots, y_{t-1})$ is a vector with the objective values observed so far;
 279 \mathbf{k}_* is a vector with the prior covariances between $f(\mathbf{x})$ and each y_i ; \mathbf{K} is a
 280 matrix with the prior covariances among each y_i , for $i = 1, \dots, t - 1$; and
 281 $k(\mathbf{x}, \mathbf{x})$ is the prior variance at the candidate location \mathbf{x} . All these quantities
 282 are obtained from a covariance function $k(\cdot, \cdot)$ which is pre-specified and
 283 receives as an input two points, \mathbf{x}_i and \mathbf{x}_j , at which the covariance between
 284 $f(\mathbf{x}_i)$ and $f(\mathbf{x}_j)$ has to be evaluated. A typical covariance function employed
 285 for BO is the Matérn function [29]. For further details about GPs we refer
 286 the reader to [53].

287 Thus, BO methods typically spend a little bit of time thinking very care-
 288 fully where to evaluate next the objective function with the aim of finding
 289 its optimum with the smallest number of evaluations. This is a very useful
 290 strategy when the objective function is very expensive to evaluate and it can
 291 save a lot of computational time. Three steps of the BO optimization process
 292 are illustrated graphically in Fig. 2 for a toy minimization problem.

293 Unlike BO methods, grid or uniform search strategies are based in a
 294 pure exploration of the search space. If we make the assumption that the
 295 objective function is smooth, doing a few evaluations in regions of the in-
 296 put space that look more promising (exploitation) is expected to give bet-
 297 ter results. In BO methods the acquisition function $\alpha(\cdot)$ balances between
 298 exploration and exploitation in an automatic way. An example of an ac-
 299 quisition function is expected improvement (EI) [54]. EI is obtained as the
 300 expected value under the GP predictive distribution for y_i , of the utility
 301 function $u(y_i) = \max(0, \nu - y_i)$, where $\nu = \min(\{y_i\}_{i=1}^{t-1})$ is the best value
 302 observed so far. That is, EI measures on average how much we will improve
 303 on the current best solution by evaluating the objective at each candidate
 304 point. An advantage of EI is that the corresponding acquisition function $\alpha(\cdot)$
 305 can be computed analytically: $\alpha(\mathbf{x}) = \sigma(\mathbf{x})(\gamma(\mathbf{x})\Phi(\gamma(\mathbf{x}) + \phi(\gamma(\mathbf{x})))$, where
 306 $\gamma(\mathbf{x}) = (\nu - \mu(\mathbf{x}))/\sigma(\mathbf{x})$ and $\Phi(\cdot)$ and $\phi(\cdot)$ are respectively the c.d.f. and
 307 p.d.f. of a standard Gaussian. EI is the acquisition function displayed in
 308 Fig. 2.

309 BO has been recently applied with success in different prediction systems
 310 for finding good parameter values. For example, it has been used to find
 311 the parameters of topic models based on latent Dirichlet allocation, support
 312 vector machines, or deep convolutional neural networks [29]. Furthermore,
 313 BO methods have also been used to optimize a logistic regression model for
 314 labelling Amazon product reviews [55], or to optimize the weights of a neural
 315 network to balance vertical poles and lengths on a moving cart [56]. Another
 316 applications of BO are found in the field of environmental monitoring, in
 317 the task of adjusting the parameters of a control system for robotics, in the
 318 optimization of recommender systems, and in combinatorial optimization
 319 [51, 52]. Finally, BO methods has been implemented in different software
 320 packages. An implementation in python is called Spearmint and is available
 321 at [57], which is the BO implementation used in this work.

322 5. Experiments and results

323 This section describes some experiments with the aim of showing the
 324 improvements obtained in the performance of the prediction system when its
 325 parameters are optimized with the Bayesian techniques introduced before.
 326 We consider a real problem of wave energy flux prediction ($P = 0.49 \cdot H_s^2 \cdot T_e$
 327 kW/m, [31]) from marine buoys. Figure 5 shows the three buoys considered
 328 in this study at the Western coast of the USA, whose data bases are obtained

329 from [58]. The objective of the problem is to carry out the reconstruction of
330 buoy 46069 from a number of predictive variables from the other two buoys.
331 Thus, 10 predictive variables measured at each neighbor buoy are considered
332 (a total of 20 predictive variables to carry out the reconstruction). Table
333 1 shows details of the predictive variables for this problem. Data for two
334 complete years (1st January 2009 to 31st December 2010) are used, since
335 complete data (without missing values in predictive and objective P) are
336 available for that period in the three buoys. These data are divided into
337 training set (year 2009) and test set (year 2010) to evaluate the performance
338 of the proposed algorithm.

339 We have divided this experimental section into two different subsections.
340 First, we show the performance of the BO techniques proposed in the op-
341 timization of the specific GGA-ELM prediction algorithm. Second, we will
342 show how the prediction performance is improved when the system is run
343 with the parameters obtained by the BO techniques, i.e. by comparing the
344 performance of the system before and after tuning the parameters with BO.

345 *5.1. Bayesian optimization of the wave energy prediction system parameters*

346 We evaluate the utility of the BO techniques described in Section 4 for
347 finding good parameters for the prediction system described in Section 3.
348 More precisely, we try to find the parameters that minimize the RMSE of
349 the best individual found by the GGA on a validation set that contains 33%
350 of the total data available. The parameters of the GGA that are adjusted
351 are the probability of mutation $p \in [0, 0.3]$, the percentage of confrontation
352 in the tournament $q \in [0.5, 1.0]$, and the number of epochs $e \in [50, 200]$.
353 On the other hand, the parameters of the ELM that is used to evaluate the
354 fitness in the GGA are also adjusted. These parameters are the number of
355 hidden units $n \in [50, 150]$ and the logarithm of the regularization constant
356 of a ridge regression estimator, that is used to find the weights of the output
357 layer $\gamma \in [-15, -3]$. Note that a ridge regression estimator for the output
358 layer weights allows for a more flexible model than the standard ELM, as the
359 standard ELM is retrieved when γ is negative and large [59].

360 We compare the BO method with two techniques. The first technique
361 is a random exploration of the space of parameters. The second technique
362 is a configuration specified by a human expert. Namely, $p = 0.02$, $q = 0.8$,
363 $e = 200$, $n = 150$ and $\gamma = -10$. These are reasonable values that are
364 expected to perform well in the specific application tackled. We set our
365 computational budget to 50 different parameter evaluations for both the BO

366 and the random exploration strategy. After each evaluation, we report the
367 performance of the best solution found. The experiments are repeated for 50
368 different random seeds and we report average results. All BO experiments
369 are carried out using the acquisition function EI and the software for BO
370 Spearmint.

371 Fig. 3 and 4 show the average results obtained and the corresponding
372 error bars for the task of predicting the wave energy flux and the task of pre-
373 dicting the wave height, respectively. Each figure shows the average RMSE
374 of each method (BO and random exploration) on the validation set as a
375 function of the number of configurations evaluated. The performance of the
376 configuration specified by a human expert is also shown. We observe that the
377 BO strategy performs best in each setting. In particular, after a few evalua-
378 tions the BO method is able to outperform the results of the human expert
379 and it provides results that are similar or better than the ones obtained by
380 the random exploration strategy with a smaller number of evaluations.

381 5.2. Estimation of the generalization performance

382 In a second round of experiments, we show the performance of the pro-
383 posed prediction system after its optimization with the BO methodology.
384 Note that after the feature selection process with the GGA-ELM approach,
385 we use an ELM and a SVR [60, 61] to obtain the final prediction of the wave
386 energy flux P and significant wave height H_s .

387 Table 2 shows the results obtained for the experiments carried out. We
388 can observe the comparison between ELM and SVR approaches in differ-
389 ent scenarios: the prediction obtained with all the features, the prediction
390 obtained with the hybrid algorithm GGA-ELM (without BO methodology),
391 and finally the prediction acquired after the application of the BO process
392 in the GGA-ELM approach. As Table 2 summarizes, we can see how the
393 hybrid GGA-ELM algorithm improves the results obtained by the ELM and
394 SVR approaches (without feature selection). In fact, the SVR algorithm im-
395 proves the values of the Pearson's Correlation Coefficient (r^2) around 75%
396 in the case of the feature selection method, against the poor 31% when all
397 features are used. Moreover, these results are improved by means of the
398 BO methodology, using ELM and SVR approaches after the GGA-ELM. In
399 the case of the ELM, we get values of the r^2 around 77% against the 71%
400 achieved with the GGA-ELM algorithm without the BO improvement. The
401 same behavior is obtained for the SVR algorithm: we have values around 78%

402 with the application of the BO methodology against the 75% obtained for
403 the GGA-ELM approach when the parameters are fixed by a human expert.

404 The results of the previous tables can be better visualized in the following
405 graphics. In Fig. 6 the temporary predictions carried out by the ELM and
406 SVR approaches are shown. We can see how the cases (c) and (d) improve
407 the approximation to the real values against the cases (a) and (b) where
408 the BO methodology is not applied. The same situation can be seen in Fig.
409 8, where the scatter plots are presented for the results obtained with and
410 without the BO methodology.

411 The same procedure is carried out in the case of the H_s . Table 3 compares
412 the results obtained in the different experiments. As it can be seen, the
413 results are improved with the use of the BO methodology with values of
414 the r^2 around 74% for the ELM and SVR predictions, against the 66% and
415 39% achieved for the ELM and SVR, respectively, with all features. The
416 GGA-ELM algorithm improves these last results, but they are not so good
417 like when we use the BO methodology. In Fig. 7 the temporary predictions
418 for the GGA-ELM-ELM, GGA-ELM-SVR, BO-GGA-ELM-ELM and BO-
419 GGA-ELM-SVR are shown. The same is done for the scatter plots, whose
420 Fig. 9, present the results mentioned above.

421 In both predictions (P and H_s) the BO methodology improves the results,
422 for this reason we can highlight the generality of the method.

423 6. Conclusions

424 In this paper we have shown how a hybrid prediction system for wave
425 energy prediction can be improved by means of Bayesian optimization (BO)
426 methodology. The prediction system is formed by a grouping genetic algo-
427 rithm for feature selection, and an Extreme Learning Machine for effective
428 prediction of the target variable, the wave energy flux in this case. After
429 this feature selection process, the final prediction of the wave energy flux is
430 obtained by means of an ELM or a SVR approach. The paper describes in
431 detail the BO methodology, and its specific application in the optimization of
432 the GGA-ELM for a real problem of wave energy flux prediction from buoys
433 data in Western California USA. The results show that the BO methodology
434 is able to improve the performance of the systems, i.e., the prediction of the
435 optimized systems is significantly better than that of the system without the
436 BO methodology applied.

437 **Acknowledgements**

438 This work has been partially supported by *Comunidad de Madrid*, un-
439 der projects number S2013/ICE-2933 and S2013/ICE-2845, and by National
440 projects TIN2014-54583-C2-2-R, TIN2013-42351-P and TIN2016-76406-P of
441 the *Spanish Ministerial Commission of Science and Technology (MICYT)*.
442 We acknowledge support by DAMA network TIN2015-70308-REDT. We ac-
443 knowledge the use of the facilities of Centro de Computación Científica de la
444 UAM.

445 **References**

- 446 [1] Z. Zheng and L. Sun, “Path following control for marine surface vessel
447 with uncertainties and input saturation,” *Neurocomputing*, vol. 177, pp.
448 158-167, 2016.
- 449 [2] L. Liu, D. Wang and Z. Peng, “Path following of marine surface vehi-
450 cles with dynamical uncertainty and time-varying ocean disturbances,”
451 *Neurocomputing*, vol. 173, pp. 799-808, 2016.
- 452 [3] F. Comola, T. Lykke Andersen, L. Martinelli, H.F. Burcharth and P.
453 Ruol, “Damage pattern and damage progression on breakwater round-
454 heads under multidirectional waves,” *Coastal Engineering*, vol. 83, pp.
455 24-35, 2014.
- 456 [4] S.W. Kim and K.D. Suh, “Determining the stability of vertical break-
457 waters against sliding based on individual sliding distances during a
458 storm,” *Coastal Engineering*, vol. 94, pp. 90-101, 2014.
- 459 [5] R.A. Arinaga, K.F. Cheung, “Atlas of global wave energy from 10 years
460 of reanalysis and hindcast data,” *Renewable Energy*, vol. 39, pp. 49-64,
461 2012.
- 462 [6] M. Esteban, D. Leary, “Current developments and future prospects of
463 offshore wind and ocean energy,” *Applied Energy*, vol. 90, pp. 128-136,
464 2012.
- 465 [7] I. López, J. Andreu, S. Ceballos, I. Martínez de Alegría and I. Ko-
466 rtabarria, “Review of wave energy technologies and the necessary power-
467 equipment,” *Renewable and Sustainable Energy Reviews*, vol. 27, pp.
468 413-434, 2013.

- 469 [8] S. Rao and S.Mandal,2005. "Hindcasting of storm waves using neural
470 networks," *Ocean Engineering*, vol. 32, pp.667-684, 2005.
- 471 [9] A.S. Bahaj, "Generating electricity from the oceans," *Renewable and*
472 *Sustainable Energy Reviews*, vol. 15, pp. 3399-3416, 2011.
- 473 [10] A.F. Falcão, "Wave energy utilization: A review of the technologies,"
474 *Renewable and Sustainable Energy Reviews*, vol. 14, pp. 899-918, 2010.
- 475 [11] M. Fadaeenejad, R. Shamsipour, S.D. Rokni, C. Gomes, "New ap-
476 proaches in harnessing wave energy: With special attention to small
477 islands," *Renewable and Sustainable Energy Reviews*, vol. 29, pp. 345-
478 354, 2014.
- 479 [12] L. Rusu, C. Guedes-Soares, "Wave energy assessments in the Azores
480 islands," *Renewable Energy*, vol. 45, pp. 183-196, 2012.
- 481 [13] L. Cuadra, S. Salcedo-Sanz, J. C. Nieto-Borge, E. Alexandre and G.
482 RodrÁguez, "Computational Intelligence in wave energy: comprehensive
483 review and case study," *Renewable and Sustainable Energy Reviews*, vol.
484 58, pp. 1223-1246, 2016.
- 485 [14] M.C. Deo and C.S. Naidu, "Real time wave prediction using neural
486 networks," *Ocean Engineering*, vol. 26(3), pp. 191-203, 1998.
- 487 [15] J.D. Agrawal and M.C. Deo, "Wave parameter estimation using neural
488 networks," *Marine Structures*, vol. 17, pp. 536-550, 2004.
- 489 [16] C.P. Tsai, C. Lin and J.N. Shen, "Neural network for wave forecasting
490 among multi-stations," *Ocean Engineering*, vol. 29(13), pp. 1683-1695,
491 2002.
- 492 [17] B. Robertson, B. Gharabaghi and K. Hall, "Prediction of incipient
493 breaking wave heights using artificial neural networks and empirical re-
494 lationships," *Coastal Engineering Journal*, vol. 57(4), 1550018, pp. 1-27,
495 2015.
- 496 [18] A. Castro, R. Carballo, G. Iglesias and J.R. Rabuñal, "Performance of
497 artificial neural networks in nearshore wave power prediction," *Applied*
498 *Soft Computing*, vol. 23, pp. 194-201, 2014.

- 499 [19] M. Zanaganeh, S. Jamshid-Mousavi and A.F. Etemad-Shahidi, “A hybrid genetic algorithm-adaptive network-based fuzzy inference system in
500 prediction of wave parameters,” *Engineering Applications of Artificial Intelligence*, vol. 22(8), pp. 1194-1202, 2009.
- 503 [20] E. Alexandre, L. Cuadra, J.C. Nieto-Borge, G. Candil-García, M. del Pino and S. Salcedo-Sanz, “A Hybrid Genetic Algorithm – Extreme
504 Learning Machine approach for accurate significant wave height reconstruction,” *Ocean Modelling*, vol. 92, pp. 115-123, 2015.
- 507 [21] L. Cornejo-Bueno, J. C. Nieto-Borge, P. García-Díaz, G. Rodríguez and S. Salcedo-Sanz, “Significant Wave Height and Energy Flux Prediction
508 for Marine Energy Applications: A Grouping Genetic Algorithm – Extreme Learning Machine Approach,” *Renewable Energy*, vol. 97, pp. 380-389, 2016.
- 512 [22] J. Mahjoobi, A. Etemad-Shahidi and M.H. Kazeminezhad, “Hindcasting of wave parameters using different soft computing methods,” *Applied
513 Ocean Research*, vol. 30(1), pp. 28-36, 2008.
- 515 [23] J. Mahjoobi and E.A. Mosabbeeb, “Prediction of significant wave height using regressive support vector machines,” *Ocean Engineering*, vol. 36(5), pp. 339-347, 2009.
- 518 [24] S. Salcedo-Sanz, J. C. Nieto-Borge, L. Carro-Calvo, L. Cuadra, K. Hessner and E. Alexandre, “Significant wave height estimation using SVR
519 algorithms and shadowing information from simulated and real measured X-band radar images of the sea surface,” *Ocean Engineering*, vol. 101, pp. 244-253, 2015.
- 523 [25] L. Cornejo-Bueno, J. C. Nieto-Borge, E. Alexandre, K. Hessner and S. Salcedo-Sanz, “Accurate estimation of significant wave height with
524 support vector regression algorithms and marine radar images,” *Coastal Engineering*, vol. 114, pp. 233-243, 2016.
- 527 [26] J.C. Fernández, S. Salcedo-Sanz, P.A. Gutiérrez, E. Alexandre and C. Hervás-Martínez, “Significant wave height and energy flux range forecast
528 with machine learning classifiers,” *Engineering Applications of Artificial Intelligence*, vol. 43, pp. 44-53, 2015.
- 529
530

- 531 [27] S.P. Nitsure, S.N. Londhe and K.C. Khare, “Wave forecasts using wind
532 information and genetic programming,” *Ocean Engineering*, vol. 54, pp.
533 61-69, 2012.
- 534 [28] M.Özger, “Prediction of ocean wave energy from meteorological vari-
535 ables by fuzzy logic modeling,” *Expert Systems with Applications*, vol.
536 38(5), pp. 6269-6274, 2011.
- 537 [29] J. Snoek, H. Larochelle, and R. P. Adams, “Practical bayesian optimiza-
538 tion of machine learning algorithms.” *Advances in neural information*
539 *processing systems*, 2012.
- 540 [30] J.C. Nieto-Borge, K. Reichert and K. Hessner, “Detection of spatio-
541 temporal wave grouping properties by using temporal sequences of X-
542 band radar images of the sea surface,” *Ocean Modelling*, vol. 61, pp.
543 21-37, 2013.
- 544 [31] Y. Goda, “Random seas and design of maritime structures,” *World Sci-*
545 *entific*, 2010.
- 546 [32] <http://www.ndbc.noaa.gov/>: National Data Buoy Center. National
547 Oceanic and Atmospheric Administration of the USA (NOAA) (accessed
548 June 29, 2016).
- 549 [33] B.G. Cahill and T. Lewis, “Wave energy resource characterization of
550 the Atlantic marine energy test site,” *International Journal of Marine*
551 *Energy*, vol. 1, pp. 3-15, 2013.
- 552 [34] E. Falkenauer, “The grouping genetic algorithm—widening the scope of
553 the GAs, *Belgian journal of operations research*,” *Statistics and Com-*
554 *puter Science*, vol. 33, pp. 79-102, 1992.
- 555 [35] E. Falkenauer, “Genetic algorithms for grouping problems,” *New York:*
556 *Wiley*, 1998.
- 557 [36] L.E. Agustín-Blas, S. Salcedo-Sanz, P. Vidales, G. Urueta and J.A.
558 Portilla-Figueras, “Near optimal citywide WiFi network deployment us-
559 ing a hybrid grouping genetic algorithm,” *Expert Systems with Appli-*
560 *cations*, vol. 38(8), pp. 9543-9556, 2011.

- 561 [37] L.E. Agustín-Blas, S. Salcedo-Sanz, E.G. Ortiz-García, J.A. Portilla-
562 Figueras and A.M. Pérez-Bellido, “A hybrid grouping genetic algorithm
563 for assigning students to preferred laboratory groups,” *Expert Systems
564 with Applications*, vol. 36, pp. 7234-7241, 2009.
- 565 [38] E.C. Brown and R.T. Sumichrast, “Evaluating performance advantages
566 of grouping genetic algorithms,” *Engineering Applications of Artificial
567 Intelligence*, vol. 18(1), pp. 1-12, 2005.
- 568 [39] T. James, E.C. Brown and K.B. Keeling, “A hybrid grouping genetic
569 algorithm for the cell formation problem,” *Computers & Operations
570 Research*, vol. 34, pp. 2059-2079, 2007.
- 571 [40] T. James, M. Vroblefski and Q. Nottingham, “A hybrid grouping ge-
572 netic algorithm for the registration area planning problem,” *Computer
573 Communications*, vol. 30(10), pp. 2180-2190, 2007.
- 574 [41] P. De Lit, E. Falkenauer and A. Delchambre, “Grouping genetic algo-
575 rithms: an efficient method to solve the cell formation problem,” *Math-
576 ematics and Computers in Simulation*, vol. 51(3-4), pp. 257-271, 2000.
- 577 [42] X. Yao, Y. Liu and G. Lin, “Evolutionary Programming made faster,”
578 *IEEE Transactions on Evolutionary Computation*, vol. 3(2), pp. 82-102,
579 1999.
- 580 [43] G.B. Huang and Q.Y. Zhu, “Extreme learning machine: theory and
581 applications,” *Neurocomputing*, vol. 70, pp. 489-501, 2006.
- 582 [44] E. Alexandre, L. Cuadra, S. Salcedo-Sanz, A. Pastor-Sánchez and C.
583 Casanova-Mateo, “Hybridizing extreme learning machines and genetic
584 algorithms to select acoustic features in vehicle classification applica-
585 tions,” *Neurocomputing*, vol. 152, pp. 58-68, 2015.
- 586 [45] S. Salcedo-Sanz, A Pastor-Sánchez, L Prieto, A Blanco-Aguilera and
587 R. García-Herrera, “Feature selection in wind speed prediction systems
588 based on a hybrid coral reefs optimization-Extreme learning machine ap-
589 proach,” *Energy Conversion and Management*, vol. 87, pp. 10-18, 2014.
- 590 [46] G. B. Huang, “ELM matlab code,” [http://www.ntu.edu.sg/home/
591 egbhuang/elm_codes.html](http://www.ntu.edu.sg/home/egbhuang/elm_codes.html)

- 592 [47] Y. LeCun, B. Yoshua and G. Hinton, “Deep learning,” *Nature*, vol.
593 521.7553, pp. 436-444, 2015.
- 594 [48] J. H. Friedman, “Stochastic gradient boosting,” *Computational Statis-*
595 *tics & Data Analysis* vol. 38.4, pp. 367-378, 2002.
- 596 [49] J. Bergstra and Y. Bengio, “Random search for hyper-parameter opti-
597 mization,” *Journal of Machine Learning Research*, vol. 13, pp. 281-305,
598 2012.
- 599 [50] J. Mockus, V. Tiesis and A. Zilinskas. “The application of Bayesian
600 methods for seeking the extremum,” *Towards Global Optimization*, vol.
601 2, pp. 117-129, 1978.
- 602 [51] E. Brochu, V. M. Cora, and N. De Freitas. “A tutorial on Bayesian
603 optimization of expensive cost functions, with application to active user
604 modeling and hierarchical reinforcement learning,” arXiv preprint arXiv,
605 pp. 1012-2599, 2010.
- 606 [52] B. Shahriari, K. Swersky, Z. Wang, R. P. Adams, and N. de Freitas.
607 “Taking the human out of the loop: A review of Bayesian optimization,”
608 *Proceedings of the IEEE*, vol. 104, pp. 148-175, 2016.
- 609 [53] C. E. Rasmussen. “Gaussian processes for machine learning,” 2006.
- 610 [54] D. R. Jones, M. Schonlau, and W. J. Welch. “Efficient global optimiza-
611 tion of expensive black-box functions,” *Journal of Global Optimization*,
612 vol. 13(4), pp. 455-492, 1998.
- 613 [55] I. Dewancker, M. McCourt and S. Clark, “Bayesian Optimization for
614 Machine Learning: A Practical Guidebook,” arXiv preprint arXiv, vol.
615 1612.04858, 2016.
- 616 [56] M. Frean and P. Boyle, “Using Gaussian processes to optimize expen-
617 sive functions,” In W. Wobcke and M. Zhang, editors, *AI: Advances in*
618 *Artificial Intelligence*, vol. 5360 of *Lecture Notes in Computer Science*,
619 pp. 258-267. Springer Berlin / Heidelberg, 2008.
- 620 [57] BO method implementation (Python): [https://github.com/HIPS/](https://github.com/HIPS/Spearmint)
621 [Spearmint](https://github.com/HIPS/Spearmint).

- 622 [58] NOAA, National Data Buoy Center: <http://www.ndbc.noaa.gov/>.
623 Last accessed 5th May 2016.
- 624 [59] A. Albert. “Regression and the Moore-Penrose pseudoinverse,” (No.
625 519.536 A5), 1972.
- 626 [60] A.J. Smola and B. Schölkopf, “A tutorial on support vector regression,”
627 *Statistics and Computing*, vol. 14, pp. 199-222, 2004.
- 628 [61] S. Salcedo-Sanz, J.L. Rojo, M. Martínez-Ramón and G. Camps-Valls,
629 “Support vector machines in engineering: an overview,” *WIREs Data*
630 *Mining and Knowledge Discovery*, vol. 4(3), pp. 234-267, 2014.
- 631 [62] David H. Wolpert, and G. M. William, “No free lunch theorems for
632 optimization,” *IEEE transactions on evolutionary computation* vol. 1.1,
633 pp. 67-82, 1997.
- 634 [63] E. Vazquez and J. Bect, “Convergence properties of the expected im-
635 provement algorithm with fixed mean and covariance functions,” *Journal*
636 *of Statistical Planning and inference*, vol. 140.11, pp. 3088-3095, 2010.
- 637 [64] C. Zhu et al, “Algorithm 778: L-BFGS-B: Fortran subroutines for large-
638 scale bound-constrained optimization,” *ACM Transactions on Mathe-*
639 *matical Software (TOMS)*, vol. 23.4, pp. 550-560, 1997.

640 **List of Tables**

641	1	Predictive variables used in the experiments.	24
642	2	Comparative results of the P estimation by the ELM and SVR 643 approaches after the feature selection by the GGA-ELM in 2010.	25
644	3	Comparative results of the H_s estimation by the ELM and 645 SVR approaches after the feature selection by the GGA-ELM 646 in 2010.	25

647 **List of Figures**

648 1 Outline of the grouping crossover implemented in the proposed
649 GGA. 26

650 2 An example of BO on a toy 1D noiseless problem. The figures
651 show a GP estimation of the objective $f(\cdot)$ over three itera-
652 tions. The acquisition function is shown in the lower part of
653 the plot. The acquisition is high where the GP predicts a low
654 objective and where the uncertainty is high. Those regions in
655 which it is unlikely to find the global minimum of $f(\cdot)$ have
656 low acquisition values and will not be explored. 27

657 3 Average results obtained for the Wave Energy Flux optimiza-
658 tion after evaluating the performance of 50 different param-
659 eters for the BO technique and a random exploration of the
660 parameter space. The performance a configuration specified
661 by a human expert is also shown for comparison. 28

662 4 Wave Height optimization average results of the performance
663 of the 50 different parameter values selected by the BO tech-
664 nique and a random exploration of the parameter space. The
665 plot also shows the performance of the parameter values sel-
666 ected by a human expert. 29

667 5 Western USA Buoys considered in this study. In red buoy
668 where the P prediction is carried out from data at blue ones. . 30

669 6 P prediction after the feature selection process with the GGA-
670 ELM approach; (a) ELM; (b) SVR; (c) ELM with Bayesian
671 optimization; (d) SVR with Bayesian optimization. 31

672 7 H_s prediction after the feature selection process with the GGA-
673 ELM approach; (a) ELM; (b) SVR; (c) ELM with Bayesian
674 optimization; (d) SVR with Bayesian optimization. 32

675 8 Scatter plots in the problem of P prediction in tackled by the
676 ELM and SVR with feature selection by the GGA-ELM; (a)
677 ELM; (b) SVR; (c) ELM with Bayesian optimization; (d) SVR
678 with Bayesian optimization. 33

679 9 Scatter plots in the problem of H_s prediction in tackled by
680 the ELM and SVR with feature selection by the GGA-ELM;
681 (a) ELM; (b) SVR; (c) ELM with Bayesian optimization; (d)
682 SVR with Bayesian optimization. 34

Table 1: Predictive variables used in the experiments.

Acronym	Predictive variable	units
WDIR	Wind direction	[degrees]
WSPD	Wind speed	[m/s]
GST	Gust speed	[m/s]
WVHT	Significant wave height	[m]
DPD	Dominant wave period	[sec]
APD	Average period	[sec]
MWD	Direction DPD	[degrees]
PRES	Atmospheric pressure	[hPa]
ATMP	Air temperature	[Celsius]
WTMP	water temperature	[Celsius]

Table 2: Comparative results of the P estimation by the ELM and SVR approaches after the feature selection by the GGA-ELM in 2010.

Experiments	RMSE	MAE	r^2
All features-ELM	3.4183 kW/m	2.4265 kW/m	0.6243
All features-SVR	4.4419 kW/m	2.8993 kW/m	0.3129
GGA-ELM-ELM	2.8739 kW/m	1.8715 kW/m	0.7101
GGA-ELM-SVR	2.6626 kW/m	1.6941 kW/m	0.7548
BO-GGA-ELM-ELM	2.5672 kW/m	1.7596 kW/m	0.7722
BO-GGA-ELM-SVR	2.4892 kW/m	1.6589 kW/m	0.7823

Table 3: Comparative results of the H_s estimation by the ELM and SVR approaches after the feature selection by the GGA-ELM in 2010.

Experiments	RMSE	MAE	r^2
All features-ELM	0.4653 m	0.3582 m	0.6624
All features-SVR	0.6519 m	0.4986 m	0.3949
GGA-ELM-ELM	0.3650 m	0.2858 m	0.7049
GGA-ELM-SVR	0.3599 m	0.2727 m	0.7056
BO-GGA-ELM-ELM	0.3324 m	0.2519 m	0.7429
BO-GGA-ELM-SVR	0.3331 m	0.2461 m	0.7396

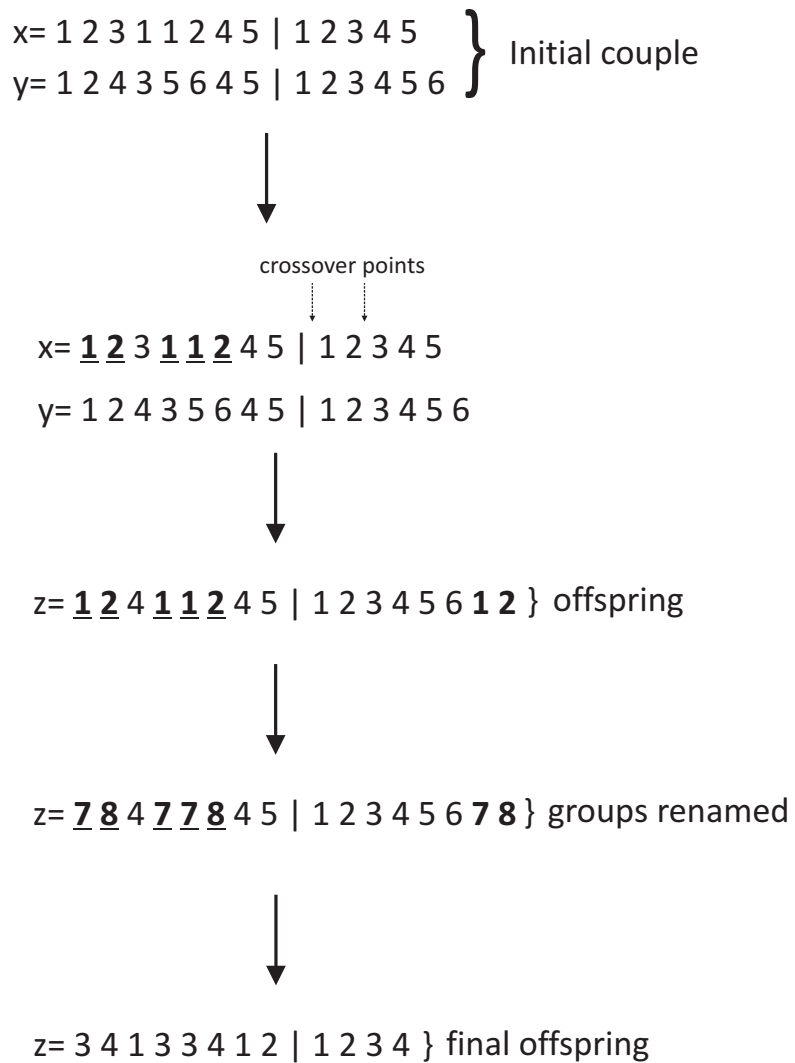


Figure 1: Outline of the grouping crossover implemented in the proposed GGA.

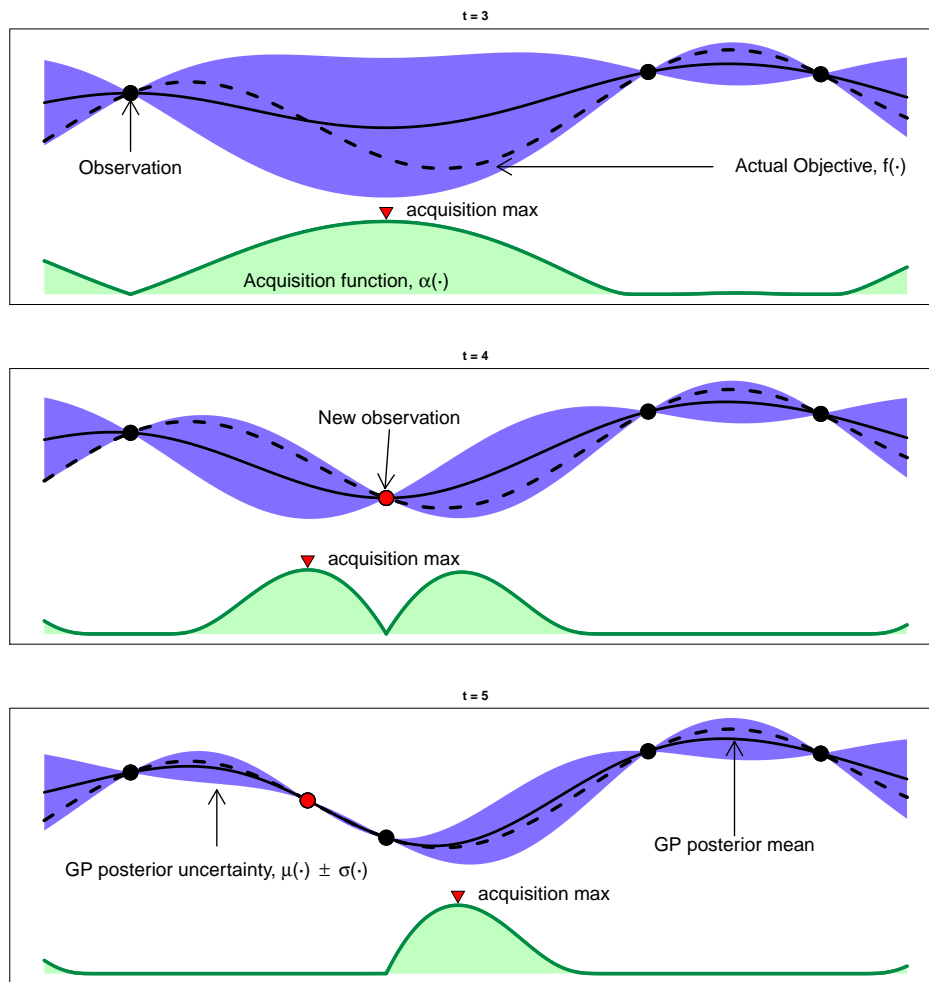


Figure 2: An example of BO on a toy 1D noiseless problem. The figures show a GP estimation of the objective $f(\cdot)$ over three iterations. The acquisition function is shown in the lower part of the plot. The acquisition is high where the GP predicts a low objective and where the uncertainty is high. Those regions in which it is unlikely to find the global minimum of $f(\cdot)$ have low acquisition values and will not be explored.

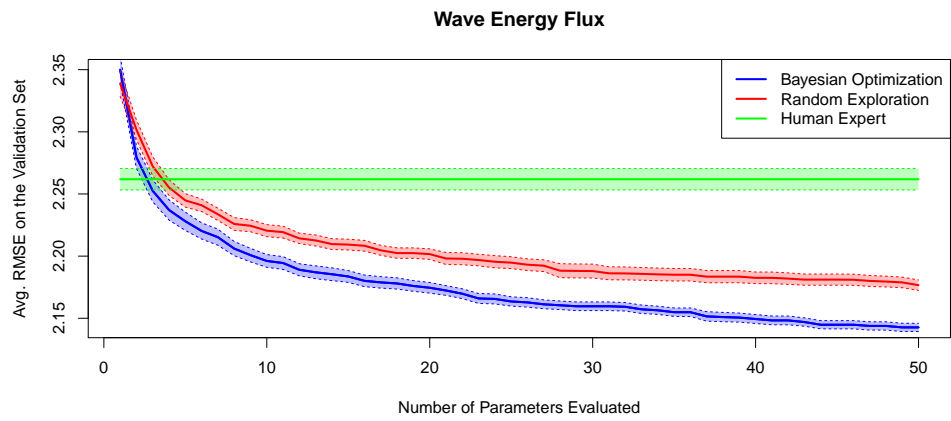


Figure 3: Average results obtained for the Wave Energy Flux optimization after evaluating the performance of 50 different parameters for the BO technique and a random exploration of the parameter space. The performance a configuration specified by a human expert is also shown for comparison.

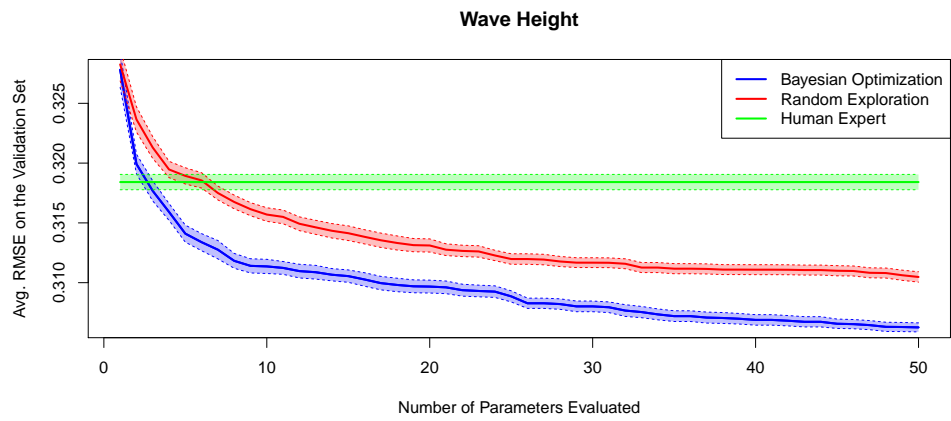


Figure 4: Wave Height optimization average results of the performance of the 50 different parameter values selected by the BO technique and a random exploration of the parameter space. The plot also shows the performance of the parameter values selected by a human expert.

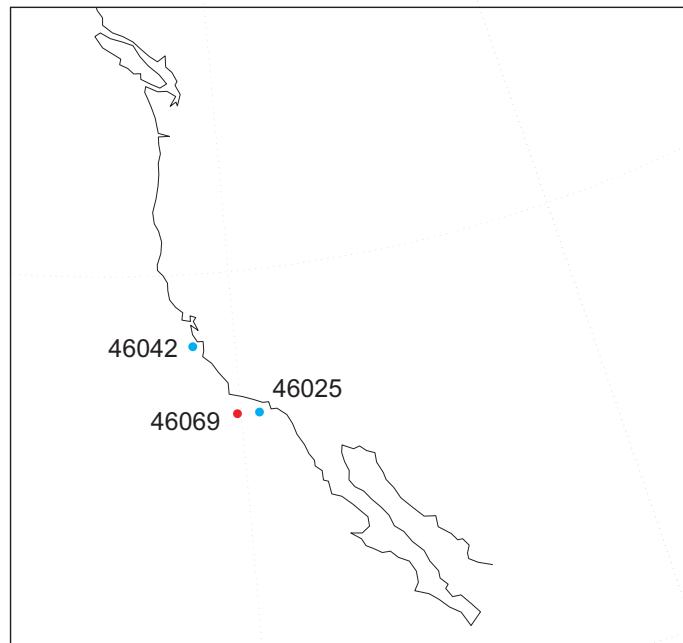


Figure 5: Western USA Buoys considered in this study. In red buoy where the P prediction is carried out from data at blue ones.

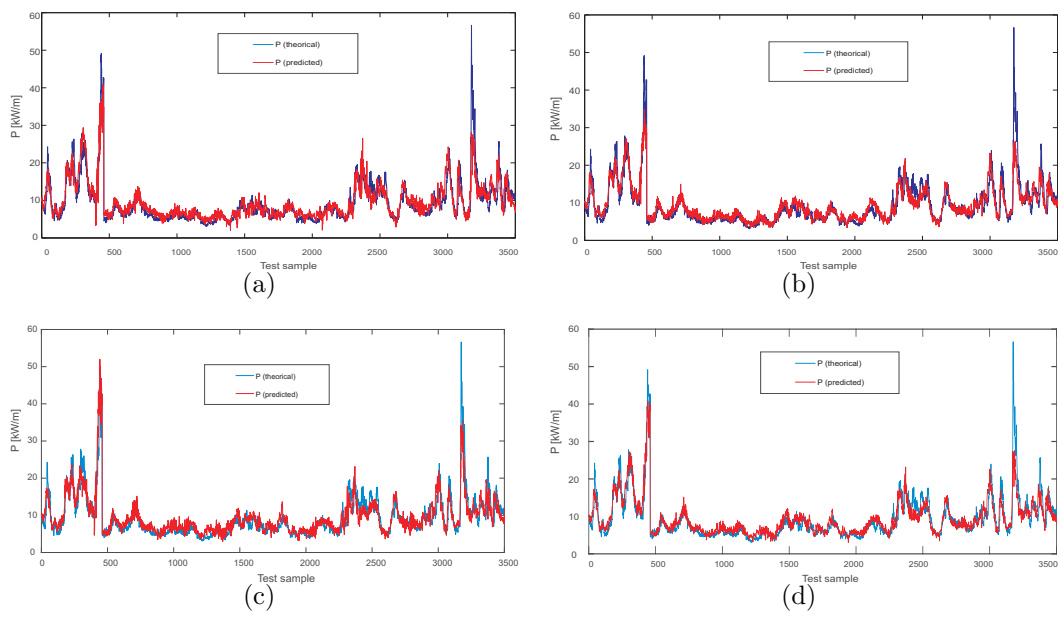


Figure 6: P prediction after the feature selection process with the GGA-ELM approach; (a) ELM; (b) SVR; (c) ELM with Bayesian optimization; (d) SVR with Bayesian optimization.

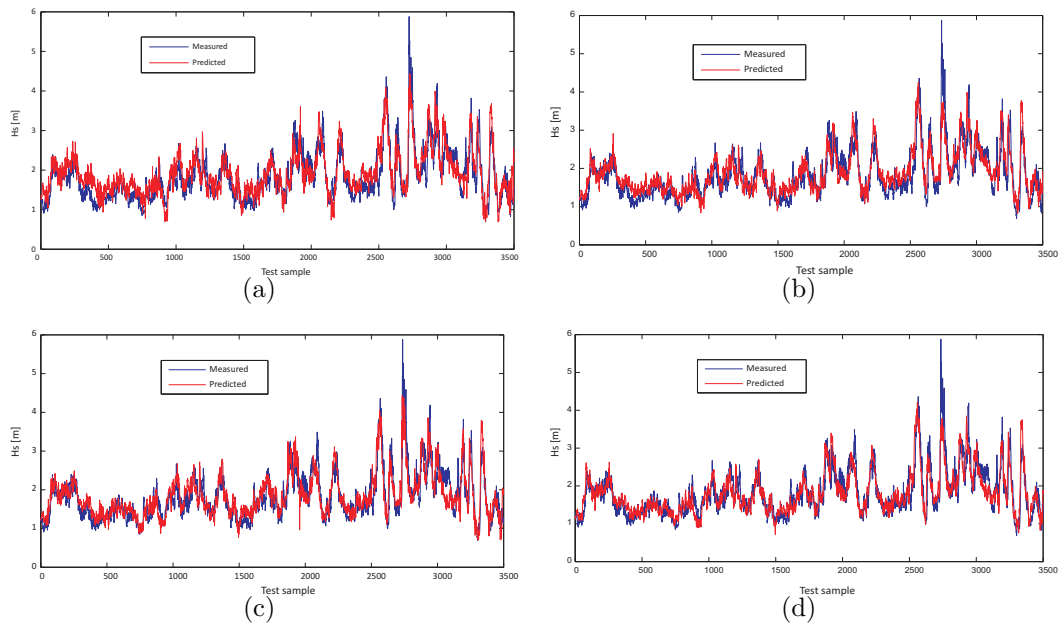


Figure 7: H_s prediction after the feature selection process with the GGA-ELM approach; (a) ELM; (b) SVR; (c) ELM with Bayesian optimization; (d) SVR with Bayesian optimization.

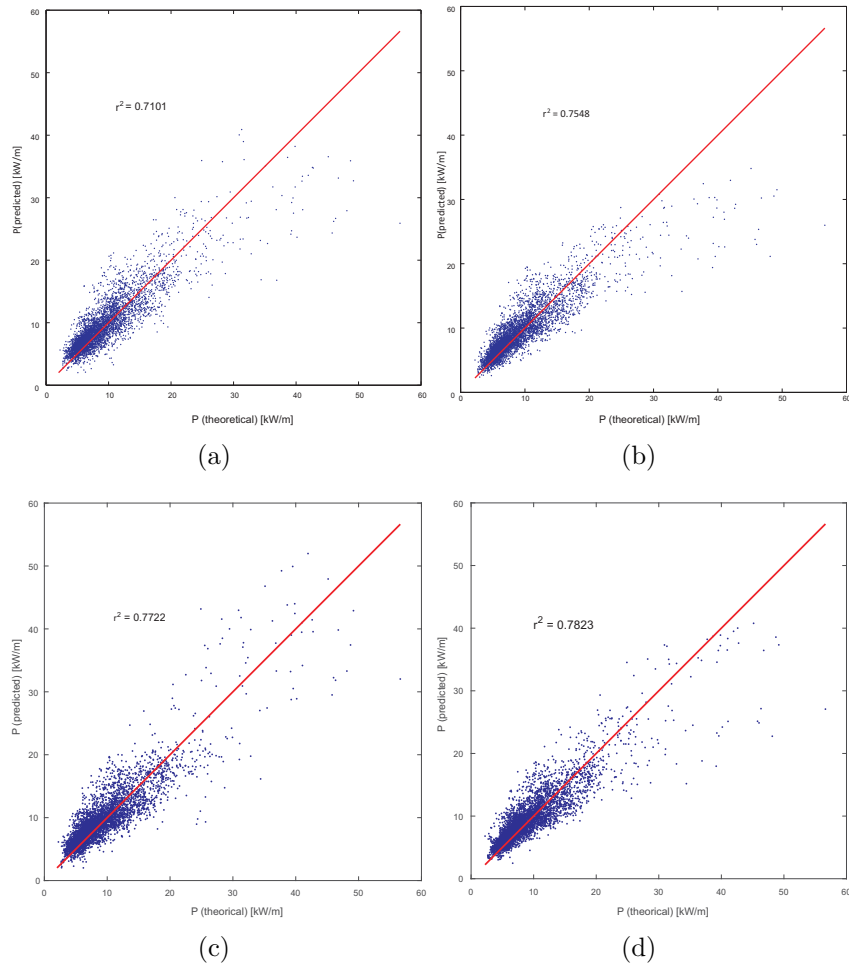


Figure 8: Scatter plots in the problem of P prediction in tackled by the ELM and SVR with feature selection by the GGA-ELM; (a) ELM; (b) SVR; (c) ELM with Bayesian optimization; (d) SVR with Bayesian optimization.

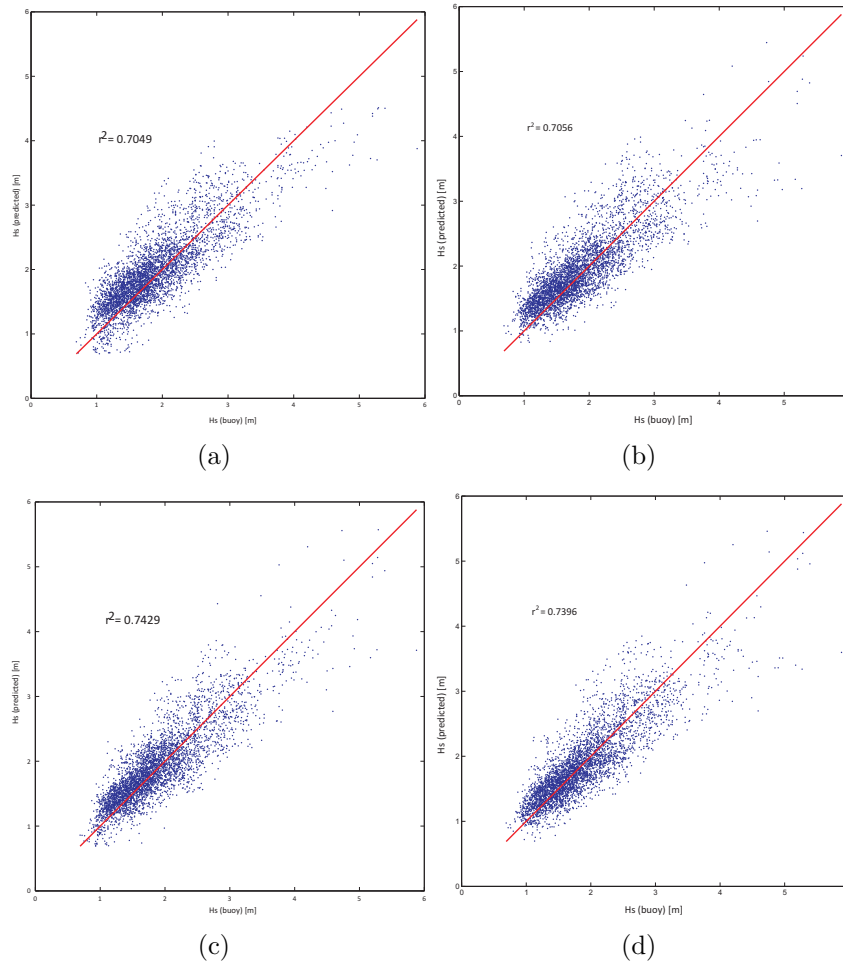


Figure 9: Scatter plots in the problem of H_s prediction in tackled by the ELM and SVR with feature selection by the GGA-ELM; (a) ELM; (b) SVR; (c) ELM with Bayesian optimization; (d) SVR with Bayesian optimization.